Spatial-anisotropy and polarized-atomic-fluorescence measurements following molecular photodissociation

H. Hemmati,* W. M. Fairbank, Jr., P. K. Boyer, and G. J. Collins
Colorado State University, Fort Collins, Colorado 80523
(Received 7 September 1982)

A study has been made of the photodissociation of the molecules NaI, TlI, $HgBr_2$, and $PbBr_2$ by polarized 193-nm ArF laser light. A significant degree of polarized fluorescence was measured from excited photoproducts Tl and HgBr. No polarization was observed in the Na and Pb fluorescence, while the Hg polarization was small. For Tl the spatial anisotropy of the dissociated atoms was also measured by atomic absorption, yielding an asymmetry parameter value of $\beta=1.2$. The best current explanation for the polarized Hg and Tl emission is that fine-structure and hyperfine-structure magnetic substates, respectively, are preferentially populated by the dissociation process.

I. INTRODUCTION

Selective population of excited levels of an atom via photodissociation of a parent molecule has been the subject of numerous investigations.[1] One example of such selectivity is the generation of laser action originating on the excited states of atoms formed following photodissociation of the parent molecules.[2] When polarized dissociating light is used, the products often have an anisotropic spatial distribution, and the subsequent atomic fluorescence may be polarized.[3] This results from preferential population of magnetic sublevels of an atom in the dissociation process.

Several attempts have been made previously to observe polarized fluorescence of atomic photofragments from NaI following photodissociation.[4,5] No polarization was observed in the emission from sodium atoms. Polarization of diatomic molecular fluorescence following photodissociation of triatomic molecules, however, has been reported for such fragment molecules as HgBr,[6] and CN.[7] Hydrogen Lyman-α radiation has also been observed to be polarized following electron-impact dissociative excitation of hydrogen molecules.[8] Recently polarized atomic emission was finally observed on the D_2 line of atomic sodium following photodissociation of Na_2 molecules.[9]

In this paper we will present results of a search for polarized fluorescence following photodissociation of NaI, TlI, $HgBr_2$, and $PbBr_2$. In the case of TlI, the anisotropy of the spatial distribution of the dissociation products was also measured. The observed polarized fluorescence from Tl is very interesting, because it can only arise from a preferential population of *hyperfine*-structure levels. This is the first time such an effect has been observed.

II. THEORY

The theory of polarized photodissociation has been developed by Zare and Hershbach[10] and Van Brunt and Zare.[3] We will first briefly review their results. The spatial distribution of the photofragments $f(\theta)$ relative to the polarization axis is in most simple cases given by[10]

$$f(\theta)=\frac{1}{4\pi}[1+\beta P_2(\cos\theta)]\ , \tag{1}$$

where $P_2(\theta)=\frac{1}{2}(3\cos^2\theta-1)$. The parameter β is called the asymmetry parameter, and θ is the angle between the polarization of the exciting light and the direction of the detector ($0\leq\theta\leq\pi$). If the molecular absorption responsible for dissociation is a parallel transition [$\Delta\Lambda$ (or Ω)$=0$, e.g., $\Sigma\rightarrow\Sigma$], $\beta=+2$, and the fragment distribution is peaked forward and backward along the direction of the electric field of the linearly polarized excitation light. For a perpendicular transition [$\Delta\Lambda$ (or Ω)$=\pm1$, e.g., $\Sigma\rightarrow\Pi$], $\beta=-1$, and the fragment distribution peaks at right angles to the polarization. In general,

$$\beta=2A_{\parallel}-A_{\perp}\ , \tag{2}$$

where $A_{\parallel}$ and $A_{\perp}$ are the fractional content of parallel and perpendicular dissociating transitions.

Polarized atomic fluorescence can occur when (1) the photodissociation process is anisotropic ($\beta\neq0$), and (2) specific magnetic sublevels of a product atom in an excited state are preferentially populated by dissociation. The degree of polarization is de-

fined by the usual expression

$$P=(I_{||}-I_{\perp})/(I_{||}+I_{\perp})\ . \tag{3}$$

We will be considering cases in which the incident light is directed along the Z axis and polarized along the X axis. The fluorescence is to be observed along the Y axis. Then $I_{||}$ and $I_{\perp}$ are the fluorescence intensities polarized along the X and Z axes, respectively. Van Brunt and Zare[3] have developed the formalism for evaluating the polarization P for cases in which different excited sublevels m are populated. The calculation takes into account the different quantization axes of the atoms (along the different atomic dissociation directions) and the Clebsch-Gordan coefficients for the possible transitions. The angular average over dissociation directions involves an integral over the spatial distribution $f(\theta)$, given by Eq. (1).[3] The results for $\Delta m=0$ and ±1 transitions are tabulated in Table I. Note that when there is no spatial anisotropy ($\beta=0$), $I_{||}=I_{\perp}$, and there is no net polarization. Using these expressions, the polarization of fluorescence from a specific upper sublevel m_F can be obtained by summing over all transitions to lower sublevels:

$$P=\frac{\sum_q [(3\beta)\delta_{q,0}-\frac{1}{2}(3\beta)\delta_{q,\pm1}]\,|\,C(F1F';m_Fq)\,|^2}{\sum_q [(10+\beta)\delta_{q,0}+\frac{1}{2}(20-\beta)\delta_{q,\pm1}]\,|\,C(F1F';m_Fq)\,|^2}\ . \tag{4}$$

The symbol $\delta_{q,\pm1}$ represents $\delta_{q,1}+\delta_{q,-1}$. A sum over lower hyperfine states F' is also needed if hyperfine transitions are not resolved optically at the fluorescence detector. In cases where there is no nuclear spin, or no nuclear spin and no electronic spin, the symbols J or L, respectively, should be substituted for F in Eq. (4).

Van Brunt and Zare argue that in general the dissociation process should be m_L selective, since the orbital angular momentum is strongly coupled to the internuclear axis in a molecule. In atoms with no nuclear or electronic spin, m_L is a good quantum number in the atom. As an example, consider the case in which one atom ends up in a ground S state and one atom in an excited $^1P_1$ state upon dissociation. If the dissociation transition is $\Sigma\rightarrow\Sigma$, the $m_L=0$ state of the $^1P_1$ excited atom should be preferentially populated. The resulting polarization of a $^1P_1\rightarrow{}^1S_0$ atomic transition is then predicted from Eq. (4) to be $3\beta/(10+\beta)$. For a $\Sigma\rightarrow\Pi$ absorption, the $m_L=\pm1$ states of the $^1P_1$ atom should be populated, instead, and $P=-3\beta/(20-\beta)$. Note that if the excited atom is in an S state, only $m_L=0$ is possible, and there can be no polarization because there was no preferential selection of excited states. Equation (4) gives $P=0$ for this case, as it should.

When the atoms have fine or hyperfine structures, it is still reasonable to expect preferential m_L selection.[3] In this case, however, a given m_L is a fractional parent of a number of different m_J or m_F states. The population in each m_J or m_F state can be calculated by squaring the appropriate Clebsch-Gordan coefficients, and an analogous expression to (4) can be obtained which has additional sums over the fractional parentage coefficients. The net result is generally to reduce the predicted polarization to a small value. Note that, if the excited state is an S state, only one m_L is still available, and again there can be no polarization observed if m_L is selected by dissociation.

Van Brunt and Zare note that sometimes the electronic or nuclear spin may be coupled strongly enough to the internuclear axis so that m_J or possibly even m_F values are preferentially selected rather than m_L. Then no fractional parentage is needed and Eq. (4) can be used directly. In this case a $^3S_1$ state could produce polarized fluorescence if $m_J=0$ or $m_J=\pm1$ states are preferentially populated. Similarly, a $^2S_{1/2}$ state with nuclear spin $\frac{1}{2}$ could produce polarized radiation if the $m_F=0$ or ±1 substates of the $F=1$ hyperfine level are selectively populated by dissociation. Note that for a $^2S_{1/2}$ state neither m_L nor m_J selection results in polarized fluorescence. Only m_F selection makes $P\neq0$ possible. An example which will be presented in this paper is Tl atoms formed in the $7s\ ^2S_{1/2}$ state by photodissociation of TlI. The only explanation for the experimentally observed fluorescence polarization is the existence of m_F selection in the dissociation process.

TABLE I. Angular integrals for $\Delta m=0,\pm1$ transitions with parallel and perpendicular polarization.

Transition type	$I_{||}$	$I_{\perp}$
$\Delta m=0$	$\frac{1}{15}(5+2\beta)$	$\frac{1}{15}(5-\beta)$
$\Delta m=\pm1$	$\frac{1}{15}(10-2\beta)$	$\frac{1}{15}(10+\beta)$

III. EXPERIMENTAL METHODS

In this paper two types of experiments will be presented. First we will discuss absorption line-shape measurements on the Tl atoms produced by dissociation of TlI. From the observed line shape the anisotropy of the spatial distribution of Tl atoms is determined. Next the method for determining the degree of polarization of the fluorescence will be described. The molecules used in these experiments were NaI, TlI, $HgBr_2$, and $PbBr_2$.

A schematic diagram of the experimental setup for absorption line-shape measurements is shown in Fig. 1. The dissociating light source was a 193-nm ArF laser (Tachisto-150XR) equipped with two Brewster angle windows. Two additional windows, placed at Brewster's angle, were introduced into the laser cavity in order to further enhance the degree of polarization of the laser beam. The output characteristics of the ArF laser were (a) a spectral width of 90 cm^{-1} centered at 193.3 nm, (b) a pulse duration of 25 nsec, and (c) a pulse energy of up to 35 mJ at repetition rates of 0.5—2 Hz. The beam was 3 mm in diameter after passing through an external iris.

The six-way cross-shaped experimental cell was made of nonmagnetic stainless steel. The distance between each pair of windows located across from each other was 8 cm. This cell was fitted with a high-vacuum valve and a separate reservoir for the TlI compound. The cell and reservoir were heated with heating tapes and kept at constant temperature to within 1 °C during measurements. The cell was always 30 °C hotter than the reservoir. Before beginning the experiments, the excitation region and the TlI reservoir were baked out at 450 °C to an ultimate pressure of better than 1×10^{-7} Torr. About 10 mg of ultrahigh purity TlI salt was placed in the reservoir. The cell was then baked under vacuum at 200 °C in order to remove any trapped impurities in the TlI solid. No higher temperatures were used due to the relatively high vapor pressures of TlI. The cell was then sealed under vacuum by closing the valve.

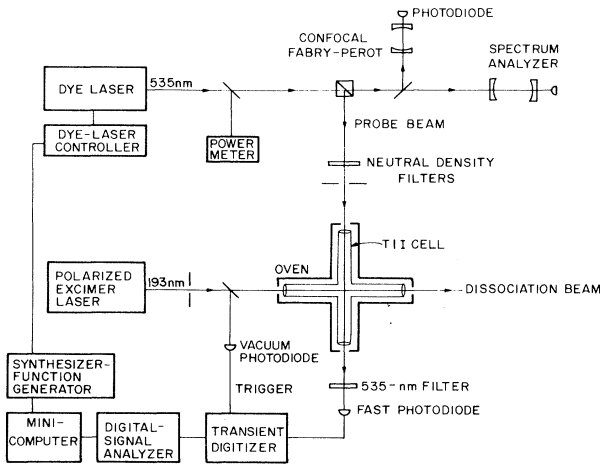

FIG. 1. Schematic of the experimental setup for absorption line-shape measurements.

The dissociation of TlL molecules by 193-nm light produces Tl atoms in the $7s\ ^2S_{1/2}$ excited state. These atoms decay to the $6p\ ^2P_{3/2}$ and $6p\ ^2P_{1/2}$ states by fluorescing with a lifetime of 7.5 nsec (Fig. 2). We monitor the buildup of population in the $6p\ ^2P_{3/2}$ state by scanning a single-frequency dye laser (CR 599-21) in 160-MHz steps across the $6p$-$7s$ absorption of 535.0 nm. The Doppler profile of the absorption is then used to determine the spatial distribution of the Tl atoms following photodissociation. Measurements were made with the 1-mm-diam dye-laser beam directed either parallel or perpendicular to the polarization of the excimer laser (excimer laser directed along Z and polarized along X; dye laser directed along X and Y).

The transmitted intensity of the dye laser was detected by a fast p-i-n photodiode (HP5082-4220). The signal from the photodiode was amplified and then digitized using a Biomation 8100 transient digitizer, used at 10 nsec per channel sample rate. The transient digitizer was externally triggered using a vacuum photodiode (Scientific Ser. Co. Model 203A), which monitored a portion (4%) of the 193-nm laser pulse. The transient digitizer was fed to a 2048-channel digital-signal analyzer (Tracor-Northern NS-570A) for accumulation of data from many laser pulses. The output of the signal averager

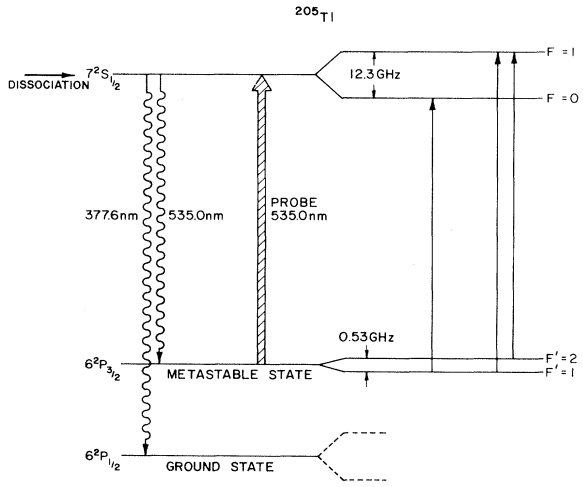

FIG. 2. Energy-level diagram for ^{205}Tl including the hyperfine states. The $7\ ^2S_{1/2}$ state is produced by dissociation of the TlI molecule. The ^{203}Tl hyperfine intervals are about 1% smaller.

was transferred to an on-line minicomputer system (HP-2100) for analysis.

A typical absorption signal at a fixed dye-laser wavelength is shown in Fig. 3. This represents an average over 64 laser pulses. The transmission first drops rapidly when the Tl atoms are created in the excited state by the 25-nsec ArF laser pulse, and decay down to the $^2P_{3/2}$ state. The transmission signal then increases again as the atoms leave the dye-laser volume. The absorption coefficient at this wavelength K_ν is given by $K_\nu=(1/L)\ln(I_0/I_T)$, where I_T is taken as the transmitted intensity at maximum absorption, and I_0 is the transmitted intensity when the atoms are all gone. The length L is approximately 3 mm, the width of the ArF laser beam. The function $K_\nu L$ is calculated on the computer after each average of 64 laser shots, and is later plotted as a function of frequency. Several curves are taken for both dye-laser probe directions.

It is important to note that, in order to be able to detect any anisotropic velocity distribution, the medium should be effectively collisionless so that any externally produced superthermal distribution is preserved. For these experiments, the TlI density was 1×10^{11} cm^{-3}, corresponding to a cell temperature of 180°C. At this TlI density, the mean-free path for Tl atoms is longer than the cell dimensions, and corresponds to a collision time longer than 100 μsec. Thus collisional effects are indeed negligible. Saturation of the absorption must be avoided. Hence the dye-laser power was kept low (at about 0.35 mW). Also, to prevent superfluorescent stimulated emission by the initial excited atoms created by photodissociation, the ArF laser flux was kept at less than 0.3 mJ/cm^2.

A schematic diagram of the experimental setup for the fluorescence polarization measurements is shown in Fig. 4. The pump laser beam, detection electronics, and experimental-cell design are the same as those described above. The atomic fluorescence was detected perpendicular to both the ArF laser-beam direction and its polarization vector. A photomultiplier tube (PMT) measured the light intensity passing through a filter and an analyzing polarizer. For each atomic emission line observed, a 10-nm full width at half maximum (FWHM) interference filter (Melles-Griot) was used. The analyzing polarizer (Melles-Griot Sheet Polarizer No. 03FPG003), with an extinction ratio of 10^{-4}, was mounted on a precision polarizer rotator. A 1P21 PMT was selected because of its fast rise time (2.6 nsec), low dark current (10 nA), and relatively high-saturation limit (0.1 mA). The fluorescence light was detected by the PMT through a 50-cm long, 12-mm-diam tube which was painted black inside in order to minimize light reflection. The acceptance angle by the PMT in such an arrangement is about 1°. No lenses were required for light collection due to the high intensity of the fluorescence.

The PMT was connected through a short, 15-cm long cable to the transient digitizer, again operating at a 10 nsec per channel sample rate. The digitizer was fed to a signal averager and from there to an on-line minicomputer system for analysis. After setting the polarization analyzer at the proper direction, the time-resolved fluorescence decay curves were obtained for emission polarized parallel ($I_{||}$) or perpendicular ($I_\perp$) to the polarization of the pump beam by averaging 128 to 256 fluorescence pulses. A typical measurement is shown in Fig. 5. Each such curve was analyzed by either finding the pulse peak height or the sum of the counts between $t_1=10$ nsec and $t_2=120$ nsec. Both methods gave similar polarization results. For each atomic line which was studied, a total of about 400 pairs of $I_{||}$ and $I_\perp$ measurements in alternating order ($I_{||}$ and $I_\perp$, then $I_\perp$

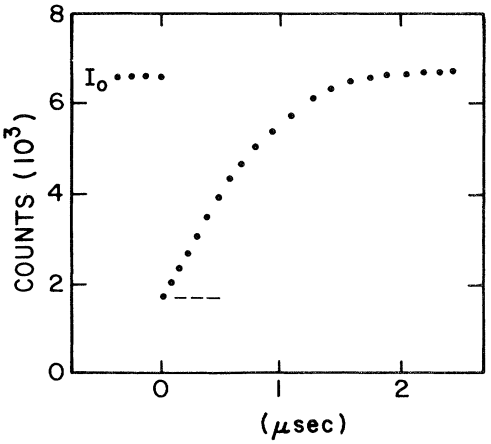

FIG. 3. A typical absorption signal for Tl($^2P_{3/2}$) atoms, following dissociation of TlI molecules ($N\simeq1\times10^{11}$ cm^{-3}).

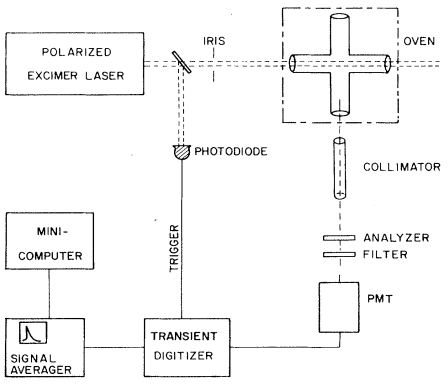

FIG. 4. Schematic diagram of the experimental setup for polarization of fluorescence measurements.

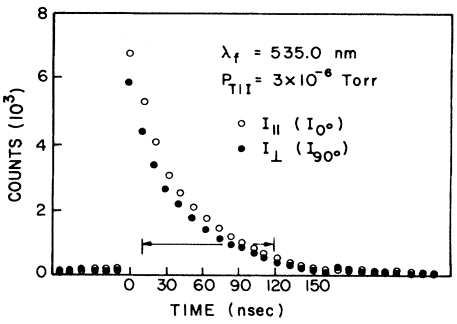

FIG. 5. Fluorescence decay curves of the polarized emission. Horizontal bar indicates the time period in which data were analyzed.

and $I_{||}$, etc.) were obtained, where each measurement at one polarization consisted of an average over 128 or 256 fluorescence pulses as explained above. Typically 16 pairs of consecutive measurements were made at a time. The degree of polarization (P) was calculated for each pair. Then all 400 P values for a given atomic line were averaged. Measurements were made on many different days to be sure that the small polarizations observed were not due to systematic effects. No variations from day to day were ever seen.

IV. LINE-SHAPE RESULTS AND DISCUSSION

The atomic Tl absorption spectra obtained after photodissociation of TlI are shown in Fig. 6. Six typical and independent spectra are presented for each probe beam direction, parallel ($||$) and perpendicular ($\perp$) to the polarization vector of the ArF pump beam. In each spectrum, the dye-laser frequency was stepped in increments of 160 MHz. In order to correct for small differences in TlI density and ArF laser energy, the amplitudes of the different spectra have been adjusted slightly by constant factors so that the highest points for all these line shapes are located at about the same level. Some of the curves were also shifted horizontally in steps of 160 MHz until the peaks best matched. This was necessary because spectra were taken on different days, and the absolute frequency of the dye laser was not measured. An uncertainty of about $\pm$ 80 MHz is introduced to the horizontal axis of each curve by this procedure.

The anisotropy predicted by Zare and Hershbach[10] is evident in the large-peak region of Fig. 6. For the $||$ direction, the peak is split into two components. This can be understood as the result of an anisotropic distribution which is peaked along the polarization axis of the ArF laser. The two components in Fig. 6 represent atoms moving mainly forward and backward along the probe laser beam. According to Eq. (1), this indicates a positive value of β. For the $\perp$ probe, a single main peak at $v=0$ is expected, which is exactly what we observe.

The reason there is a second smaller peak on the left in Fig. 6 is that thallium has two isotopes: ^{205}Tl and ^{203}Tl, with abundances of 70.54 at. % and 29.46 at. %, respectively. The displacement of the two peaks is about equal to the known isotope shift for thallium, 1.7 GHz.[11,12] Actually, since both isotopes have nuclear spin $I=\frac{1}{2}$, there are three hyperfine transitions possible: $F'=1\rightarrow F=1$, $F'=2\rightarrow F=1$, and $F'=1\rightarrow F=0$ (see Fig. 2). On a larger 30-GHz scan all three transitions can be seen. Figure 6 shows only the $F'=1\rightarrow F=0$ component. This hyperfine transition is convenient to use for analysis because optical pumping cannot occur in this case. Thus saturation due to optical pumping is not a problem.

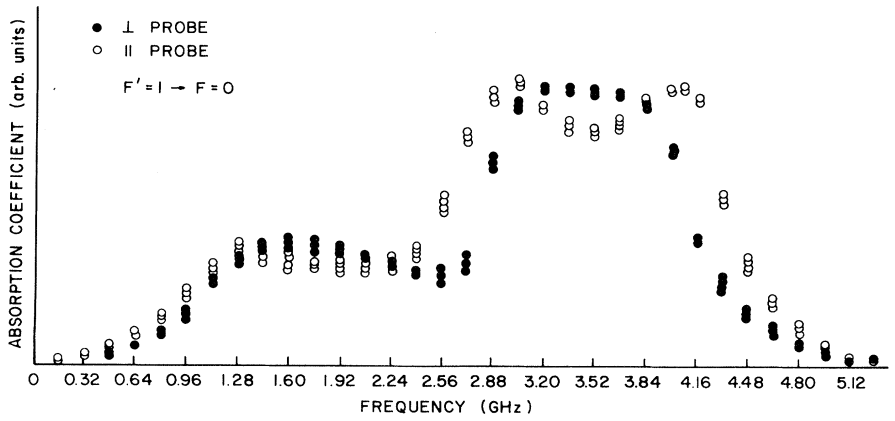

FIG. 6. Absorption line-shape spectra obtained experimentally by probing the Tl($^2P_{3/2}$) atoms in directions parallel and perpendicular to the polarization vector of the pump beam. Six independent sets of measurements are shown for each probe direction. Large bump on the right is due to ^{205}Tl(70.54 at. %). Smaller bump on the left is due to ^{203}Tl(29.46 at. %).

The theoretical expressions for the Doppler line-shape function of photodissociated atoms have been derived by Zare and Hershbach.[10] Their analysis takes into account the distribution of velocity components due to an anisotropic dissociation probability as well as the broadening due to the initial thermal-velocity distribution of the molecules. We have assumed that in the molecule center-of-mass frame of reference each pair of atoms is given the same kinetic energy $h\nu - D_0 - E$ and that the angular distribution of products is given by Eq. (1). For the TlI experiment, the incident photon energy is $h\nu = 6.413$ eV, the dissociation energy is $D_0 = 2.73$ eV,[13] and the energy left in the excited Tl atom is $E = 3.283$ eV. This leaves 0.40 eV to be shared between the Tl and I atoms. According to conservation of momentum, the Tl atoms will all get 0.135-eV kinetic energy in the center-of-mass frame. This corresponds to a Tl atom velocity of $v = 3.79 \times 10^4$ cm/sec. At 190°C the most probable thermal velocity of the TlI molecules is $\alpha = 1.92 \times 10^4$ cm/sec. In the notation of Ref. 10, the ratio of these two velocities is $n = 1.98$. In their analysis, Zare and Hershbach also included the effects of the initial thermal population of a variety of rotational and vibrational states. Since the potential curves of TlI are not well known, we had to ignore such effects in our calculations. One might expect that the rotational and vibrational states of TlI initially populated might be spread over an energy interval on the order of kT, which in this case is 0.040 eV. Since this is only 10% of the kinetic energy of dissociation, the errors involved in this approximation should be small. The 0.011-eV bandwidth of the ArF laser can be neglected for the same reason.

The theoretical line-shape functions incorporating the known Tl isotope shift and the known isotope abundances are plotted for several possible values of the asymmetry parameter β in Figs. 7 and 8. The fit is quite good in both figures for a value of $\beta = 1.2$. The only differences between theory and experiment are in the wings of the lines. The slight amount of extra broadening in the experimental curves is probably representative of the initial spread of population over vibrational and rotational states of TlI, which was neglected in the theory. A slightly better fit was obtained by adjusting the isotope shift to 1.74 GHz and the dissociation energy to $D_0 = 2.78$ eV.

From the observed asymmetry parameter $\beta = 1.2$ the fractions of parallel and perpendicular transitions responsible for producing $7s\ ^2S_{1/2}$ Tl atoms can be calculated using Eq. (2): $A_{\parallel} = (\beta + 1)/3 = 0.73$ and $A_{\perp} = 1 - A_{\parallel} = 0.27$. The only state expected to be in this region which can give a parallel contribution is a $^1\Sigma^+_{0+}$ state. Thus we can conclude from our results that such a state is responsible for most of the observed dissociation into $7s$ Tl atoms. The smaller perpendicular contribution could come from either $^3\Pi_1$ or $^3\Sigma^+_1$ states.

V. POLARIZATION OF FLUORESCENCE RESULTS AND DISCUSSION

The results of our measurements of the polarization of fluorescence from excited atomic and molecular products following photodissociation of TlI, $HgBr_2$, $PbBr_2$, and NaI are summarized in Table II. In two of the cases, NaI and $PbBr_2$, no significant atomic polarization was observed. The NaI result is in agreement with previous experiments[4,5] which also failed to detect any polarized Na fluorescence.

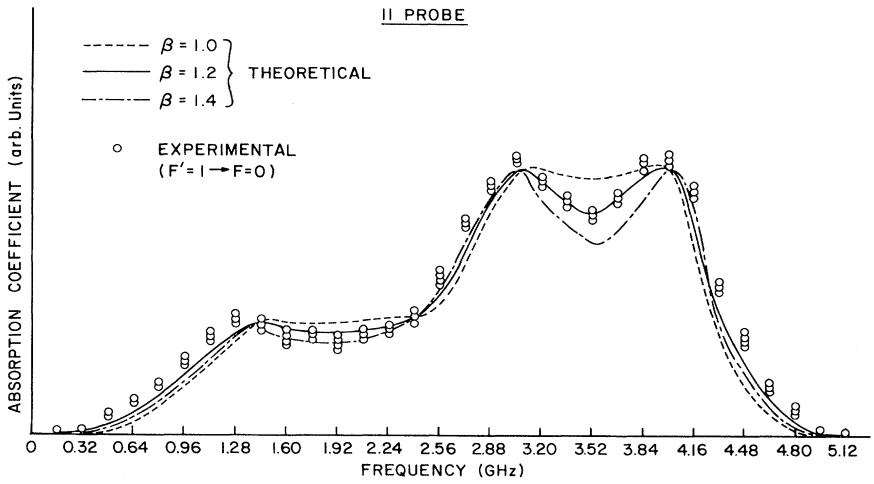

FIG. 7. A comparison of the experimentally obtained line-shape spectra for probe in the parallel direction to the theoretical line-shape functions at various values of the asymmetry parameter β.

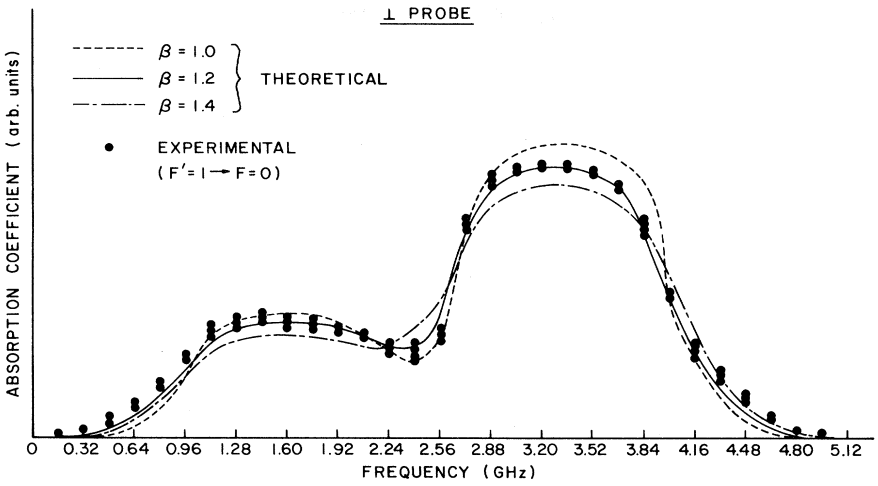

FIG. 8. A comparison of the experimentally obtained line shape for probe in the perpendicular direction to the line-shape functions at various values of the asymmetry parameter β.

The explanation for this result is that in NaI a variety of Σ and Π dissociative states are close together. Therefore, very little spatial anisotropy is produced by dissociation ($\beta \approx 0$), because transitions occur equally well to states of each symmetry. The $PbBr_2$ results are consistent with the very small polarizations predicted by theory. No conclusions on β can be obtained in this case.

A significant degree of polarization was observed for excited Tl, Hg, and HgBr following photodissociation of TlI and $HgBr_2$. The large polarization of HgBr, $+0.135 \pm 0.004$, agrees well with the theoretical value[6] of 0.143 and the previous experimental result (also using an ArF laser) of 0.115 ± 0.010.[6] This experiment was done as an extra check on our method of polarization measurements. The good agreement gave us confidence that our error analysis was satisfactory.

The two successful atomic polarization experiments, Hg and Tl, are quite interesting because in

TABLE II. The measured and calculated degrees of polarization (P) of atomic fluorescence.

Parent molecule	Excited-state product (wavelength)	Observed polarization (P)	Calculated polarization (P) $\beta=2$	Calculated polarization (P) $\beta=-1$	Sublevel populated	Remarks
TlI	$Tl(^2S_{1/2})$ (535.0 nm)	-0.043 ± 0.003	-0.077	$+0.037$	$F=1\ M_F=0$	$P=0$ for M_L or M_J population
			$+0.037$	-0.019	$F=1\ M_F=\pm 1$	
			0	0	$F=0\ M_F=0$	
$HgBr_2$	$Hg(^3S_{1/2})$ (435.8 nm)	$+0.018 \pm 0.008$	$+0.14$	-0.077	$M_J=\pm 1$	$P=0$ for M_L population
			-0.27	$+0.158$	$M_J=0$	
	$HgBr(^2\Sigma^+)$	$+0.135 \pm 0.004$	0.143			
$PbBr_2$	$Pb(^3P_1)$ (405.8 nm)	$+0.0085 \pm 0.006$	-0.03	$+0.015$	$M_L=0$	
			$+0.015$	-0.007	$M_L=1$	
NaI	$Na(^2P_{3/2})$ (589.0 nm)		$+0.27$	-0.158	$M_L=0$	
		-0.003 ± 0.004	-0.158	$+0.073$	$M_L=\pm 1$	
	$Na(^2P_{1/2})$ (589.6 nm)		0	0	$M_L=0$	
			0	0	$M_L=\pm 1$	

both cases the excited atomic state is an S state. As stated in our theoretical discussion above, preferential population of m_L states is generally expected. Under this assumption no polarization can exist if the excited state is an S state. The Hg result apparently shows a small asymmetry (on the order of 10%) in the population of m_J sublevels in Hg following photodissociation. Since the Doppler line shape was not measured for Hg, it is not known whether β is positive or negative. Hence we cannot determine which sublevel has the larger population. The theoretical analysis is complicated by the fact that the exact mechanism for production of excited Hg atoms is not known. The most probable reaction is a second-step photodissociation of HgBr following the photodissociation of $HgBr_2$ into HgBr and ground state Br.[14]

The TlI result is even more surprising. Since the excited state is a $^2S_{1/2}$ state, there can be neither preferential population of m_L nor m_J states. The only way to account for the observed result $P=-0.043\pm0.003$ is the selective population of *hyperfine* states. Using the asymmetry parameter measured by atomic absorption $\beta=1.2$, the predicted polarizations for selective population of the ($F=1$, $M_F=0$), ($F=1$, $M_F=\pm1$), and ($F=0$, $M_F=0$) excited states of Tl are -0.046, $+0.022$, and 0, respectively. It is remarkable that the former value agrees so closely with the experimental result. This indicates that almost all of the population is in the $F=1$, $M_F=0$ hyperfine substate of the $7s\ ^2S_{1/2}$ level. This result is especially surprising in light of the fact that the hyperfine splittings in the atom are only 0.41 and 0.017 cm^{-1} for the excited $7s\ ^2S_{1/2}$ and $6p\ ^2P_{3/2}$ metastable states, respectively. Molecular hyperfine splittings might be expected to be of the same order of magnitude. Since the photodissociation laser has a bandwidth of 90 cm^{-1}, it is hard to see how selective hyperfine-state pumping could occur. It would be very interesting to check this result by hyperfine-state resolved absorption from the $7s$ state to a higher state in Tl.

VI. ERROR ANALYSIS

Since the observation of polarized fluorescence from Tl was very unusual, we were especially careful in our analysis of possible errors in the experiment. In all cases the statistical errors were small because a large amount of data was taken. For example, about 400 pairs of measurements of $I_{||}$ and $I_\perp$ with alternating polarization were taken on a number of different days. The degree of polarization calculated for each pair of measurements ranged only from -0.052 to -0.0310. No single pair of measurements ever gave zero or positive polarization. A conservative statistical error limit for 200 pairs of these measurements, three standard deviations of the mean (99.7% confidence level), is only ±0.0025.

Possible systematic errors in the polarization measurement include slow drifts in the TlI density and the ArF laser energy, incomplete polarization of the ArF laser, polarization effects of the optics used in the experiment, the effect of external errors in setting the analyzer, polarized emission from background gases in the cell, and magnetic fields. These sources and the estimated error limits for each are listed in Table III and are discussed in detail below.

Since the fluorescence intensity is proportional to both the ArF laser power and the TlI density, slow variations in these quantities could cause large systematic errors. At 180 °C, a temperature change of 1 °C causes a 7.5% change in the TlI density. If $I_{||}$ and $I_\perp$ measurements were made alternately while the TlI density or laser power was steadily increasing, the second measurement in a pair would always be systematically enhanced. To avoid this problem, we alternated the order within the pairs. One pair consisted of $I_{||}$ followed by $I_\perp$, the next pair was $I_\perp$ followed by $I_{||}$, etc. Then when an average is taken over all pairs, these slow drift effects should cancel. Since the maximum variation in P for individual pairs was only about ±0.010, the systematic error in the average due to this effect should be less than ±0.001.

The polarization of the ArF laser was not perfect. In fact, it varied significantly from shot to shot. We made ten consecutive measurements of the laser polarization with each measurement consisting of an average of 128 laser pulses for each polarization, as in the $I_{||}$ and $I_\perp$ measurements. The average polarization was found to be 0.957 with a standard deviation for the ten measurements of 0.003. The sys-

TABLE III. Sources of errors in the Tl fluorescence polarization experiment.

Source of contrib.	Maximum contrib. to P error
Reservoir temperature and ArF power	$<\pm0.001$
Pump polarization uncertainty	±0.0001
Optics	±0.001
Background atomic and molecular fluorescence	$<\pm0.0001$
Uncertainty in setting the analyzer	±0.0019
Stray light external magnetic field	$<\pm0.001$
Statistical	±0.002
Total error limit	±0.003

tematic effect of the 95.7% polarization is to reduce the observed polarizations by 4.3% from what they would have been had the ArF laser polarization been perfect. This small correction was made to the data in the calculation of Table II. The remaining 0.3% uncertainty in the pump polarization produces a negligible (e.g., ± 0.0001 for Tl) uncertainty in the fluorescence polarizations measured. Similar measurements were made before and after the entrance window to the cell. No polarization effects at 193 nm due to the cell entrance window were observed.

The polarization effects of the fluorescence detection optics, i.e., the sapphire output window of the cell, the interference filters, and the photomultiplier tube itself, were tested by shining three different light sources down the fluorescence path. First, linearly polarized Tl and Hg lamps and a polarized He-Ne laser were used with the corresponding interference filters. Ten pairs of $\|$ and $\perp$ measurements each averaged for 10 min, yielded $P = 0.998 \pm 0.002$. Physical rotation of each component caused no change in the result. From these measurements we can conclude that no significant birefringent effects exist in the optics which cause detectable rotation of the polarization to an uncertainty of 0.2%. Since the polarizations observed are small, the optical rotation uncertainty is negligible in this experiment. The effect of slightly different transmission for different polarizations in the fluorescence optics was tested by using an unpolarized Tl lamp ($P = +0.020$). Each optical component—including the windows, collimator analyzer, and filter—was inserted one by one and rotated. In no case was any transmitted polarization change detected to an uncertainty of ± 0.001. Rotating the lamp by 90° changed the transmitted polarization from $+0.020$ to -0.020 as it should. Thus the uncertainty in P from the optics is ± 0.001. Finally, the errors in setting the analyzers are small because the initial alignment was very careful and precision rotators were used. Assuming a 1° uncertainty in the orientation of the $I_{\|}$ position relative to the pump polarization results in a 1.7% uncertainty in the P measurement, or ± 0.0008 in the Tl experiment. Assuming a 0.1° uncertainty in the location of the $I_{\|}$ position relative to the $I_{\perp}$ position results in an absolute error of ± 0.0017. Adding these errors in quadrature gives a total analyzer setting uncertainty of ± 0.0019.

Additional sources of errors are stray room light, stray pump light, and fluorescence from other cell contaminants. The stray room light was eliminated by shielding the detector and by doing all experiments in a completely darkened room. The stray pump light is not a problem because the detector window does not transmit 193-nm photons. In order to be sure, polarization measurements for 256 laser pulses were done when the cell was void of metal halide. No polarization of the dark current and stray light signal was observed with an uncertainty of ± 0.001. The systematic error contribution of stray light to the fluorescence measurements will therefore be negligible, since the peak fluorescence was typically 10^4 times larger than the background level. We also measured the fluorescence spectra of each species near the resonance line of interest using a spectrometer in order to look for atomic or molecular emission from background gases. In no case was any other fluorescence line or band found in the fluorescence-line region of the desired species. The systematic error from this source is probably much less than ± 0.0001, since the impurities would be unlikely to have 100% polarized emission.

The final source of systematic error, external magnetic fields, cannot be evaluated because the theoretical effects of magnetic fields on the polarization have not been determined. We measured polarization with and without the heating tapes on, and found no significant difference. The average field in the interaction region was measured by a Gaussmeter to be 0.5 G, both with and without the heating tapes. This is probably mainly the magnetic field of the Earth.

A summary of all systematic errors for the TlI experiment is presented in Table III. The total error of ± 0.003 for the TlI experiment is derived by adding all errors in quadrature. The errors for the other experiments quoted in Table II are obtained in a similar manner.

VII. CONCLUSIONS

In summary, by atomic absorption we have measured the anisotropy in the spatial distribution of the products of the photodissociation of TlI. It was concluded that about $\frac{3}{4}$ of the observed dissociation is due to a $^1\Sigma^+_{0+} \rightarrow {}^1\Sigma^+_{0+}$ transition. In addition, we have measured the polarization of the fluorescence emitted by excited products of the photodissociation of TlI, NaI, $HgBr_2$, and $PbBr_2$. In the two atomic cases where polarization is most likely, Na and Pb, no significant polarization was observed. The observed polarization from S states of Hg and Tl apparently indicates the selective population of individual magnetic fine- and hyperfine-structure states, respectively. This result is new and quite surprising, and it warrants further investigation.

ACKNOWLEDGMENT

One of us (G.C.) would like to acknowledge receipt of an Alfred Sloan Foundation Fellowship.

*Present address: National Bureau of Standards, Frequency and Time Standards Group, Boulder, Colorado 80302.

[1]S. R. Leone, in *Dynamics of Excited State, Advances in Chemical Physics,* edited by K. Lawley (Wiley, New York, 1981), Vol. 50 p.255.

[2]D. J. Ehrlich and R. M. Osgood, Jr., IEEE J. Quant. Electron QE-16, 257 (1980).

[3]R. J. Van Brunt and R. N. Zare, J. Chem. Phys. 48, 4304 (1968).

[4]A. C. G. Mitchell, Z. Phys. 49, 228 (1928).

[5]M. Hanson, J. Chem. Phys. 47, 4773 (1967).

[6]J. Husain, J. R. Wiesenfeld, and R. N. Zare, Chem. Phys. Lett. 72, 2479 (1980).

[7]E. D. Poliakoff *et al.,* Chem. Phys. Lett. 65, 407 (1979).

[8]G. N. Dunn and L. J. Kieffer, Phys. Rev. 132, 2109 (1963).

[9]E. W. Rothe, U. Krause, and R. Duren, Chem. Phys. Lett. 72, 100 (1980).

[10]R. N. Zare and D. Hershbach, Proc. IEEE 51, 173 (1963).

[11]C. J. Shuler *et al.,* J. Opt. Soc. Am. 52, 501 (1962).

[12]A. Gallagher and A. Lurio, Phys. Rev. 136, A87 (1964).

[13]K. P. Huber and G. Herzberg, *Constants of Diatomic Molecules* (Van Nostrand Reinhold, New York, 1979).

[14]T. A. Cool, J. A. McGarvey, and C. Erlandson, Chem. Phys. Lett. 58, 108 (1978).